

# Probing-Based Inertia Estimation Method Using Hybrid Power Plants

Zhihao Jiang<sup>1</sup>, He Yin<sup>1</sup>, Hongyu Li<sup>1</sup>, Yilu Liu<sup>1,2</sup>  
1 - University of Tennessee, 2 – Oak Ridge National Laboratory  
Knoxville, USA

Jin Tan, Andy Hoke  
National Renewable Energy Laboratory  
Denver, USA

Brad Rockwell, Cameron Kruse  
Kauai's Island Utility Cooperative  
Hawaii, USA

**Abstract**—With the displacement of synchronous generation by inverter-based resources (IBRs), power systems could face the challenge of reduced inertia since IBRs do not inherently contribute to system inertia. Therefore, there is rising interest in monitoring system inertia in real-time applications for situational awareness. In addition, there is a growing number of IBRs that provide fast frequency responses (FFR) in the form of synthetic inertia and P-f droop. It is desirable to quantify the contribution of these FFR controls as equivalent inertia. This paper proposes a probing-based inertia estimation method using a PV-battery hybrid power plant in the Kauai island power system. The method is validated under different operating conditions.

**Index Terms**—inverter-based resources, inertia estimation, probing signal, hybrid power plant

## I. INTRODUCTION

Decarbonization goals and falling costs of renewable generators have precipitated the retirement of conventional fossil-fueled synchronous generation and the integration of inverter-connected renewable generation. With fewer synchronous units online, power systems could experience the challenges of reduced inertia since inverter-based resources (IBRs) do not inherently contribute to system inertia due to the lack of rotational mass. System frequency could experience high-magnitude deviations under low-inertia conditions and could lead to increased under-frequency load shed operations. Therefore, it is important to monitor real-time inertia to maintain grid reliability.

In past studies, there have been a lot of research on inertia estimation methods in power systems. These methods could be categorized into dispatch-based methods, event-driven methods [1] [2] [3] [4] [5] [6] [7] [8] [9], ambient signal-based methods [10] [11] [12] [13] [14] [15] [16] and probing based methods. Dispatch-based methods estimate system inertia by summing up all the inertia contribution from dispatched synchronous generation using information from energy management systems (EMS). These methods are easy to implement but it does not consider the contribution from other resources in the system, including load inertia, FFR from IBRs,

and other components that could provide artificial inertia [17] [18].

Event-driven inertia estimation methods utilize recorded events by wide-area monitoring devices. System inertia is estimated based on the known size of the event and the initial Rate of Change of Frequency (RoCoF) calculated from measurements. The drawback of this type of method is its requirement on the availability of the event and the MW information of the event size. In addition, the estimated inertia from recorded events is affected by the system operating conditions and settings of FFR from IBRs at the time of the event. Therefore, it is difficult to implement the approach for real-time monitoring purposes.

Ambient-based methods do not rely on recorded events to estimate inertia. Instead, a linear model is normally identified between system frequencies and load variations during normal conditions using system identification techniques. System inertia is then estimated by simulating the step responses of the identified model or directly extracted from the model coefficients. To realize real-time inertia monitoring, the application of ambient-based methods depends on the availability of measurements of ambient load variations within the study area, which could be approximated by the measurements of generation and tie-line power interchange of the researched area. In addition, there are some challenges in data processing techniques when extracting ambient noise from active power and frequency measurements.

Another real-time inertia monitoring method is the probing-based method. Different from ambient-based methods, probing-based methods inject active power into the system and identify the linear model between the probing signal and measured system frequency responses. System equivalent inertia could then be extracted from the identified model. In previous efforts, devices that inject probing signal could require extra installment and operating costs. In [19] supercapacitors are installed in the UK system to generate probing pulses into the system. In this work, instead of adding devices that are dedicated for probing injection, Battery Energy Storage System (BESS) in the Kauai island system are used to inject active power variations into the system. The idea

is to use small power changes from BESS to slightly alter the frequency and calculate real-time inertia based on grid frequency response. The probing signal is small compared to the regular output power provided by BESS in hybrid plants, so this approach can be stacked with other BESS-based grid services.

The rest of the paper will be organized as follows. Section II will introduce the general procedure of the proposed probing-based inertia estimation method. Section III will discuss some factors that may be encountered in field applications that could affect the performance of the proposed inertia estimation method. Section IV will present case study results using the simulation model of Kauai island system under different conditions. Section V will summarize the key findings, conclusions and future work.

## II. PROCEDURE OF PROBING-BASED INERTIA ESTIMATION

### A. Inertial response

In response to system events that causes active power imbalances between load and generation, synchronous generation could inherently exchange kinetic energy, causing synchronous machines to change speed. This ability to oppose changes in system frequency using the stored rotational energy is called inertial response. Synchronous machines could release the energy spontaneously and immediately to maintain the active power balance in the system.

The relationship between the active power generation and the rotating speed (frequency) of a synchronous machine could be described using the well-known swing equation, as shown in (1).

$$2H \frac{df}{dt} = P_m - P_e - D\Delta f \quad (1)$$

where  $f$  is the machine bus frequency,  $P_m$  is the mechanical power provided by the prime mover,  $P_e$  is the electrical power generated by the machine,  $D$  is the damping coefficient of the generator,  $H$  is the inertial constant of the machine.

Following an event that causes active power imbalance in the system, thanks to the inertial response of the synchronous generation, system frequency will not change instantaneously, according to (1). The initial RoCoF is limited by the inertial response and the damping of the generator.

### B. Probing-based inertia estimation

Based on the swing equation, system inertia could be estimated by measuring frequency dynamics and power imbalances in the system. Since inertial response is much faster than the mechanical dynamics involved with the change of mechanical power,  $P_m$  could be considered as constant in the estimation.

Different from [19], this study proposes a probing-based inertia estimation method using the PV-BESS plants on Kauai

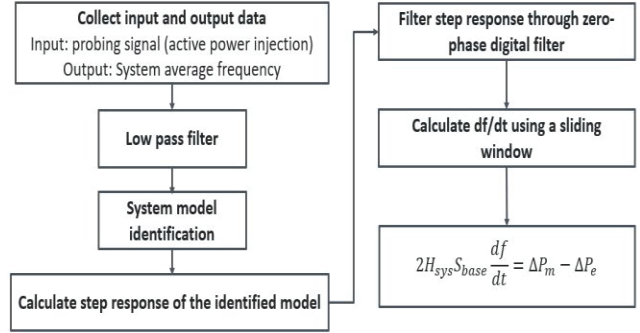


Figure 1 General procedure of probing-based inertia estimation

island. A general procedure of the proposed method is shown in Figure 1. Active power is injected into the system and frequency dynamics are measured. After some data preprocessing techniques, including low-pass filtering and down-sampling, a linear model is estimated using system identification techniques. When estimating the inertia of a single machine, the input of the model will be the active power generation of the machine and the output will be the generator bus frequency. When estimating total system inertia, the input will be the total power imbalance of the system, which equals the injected probing active power, and the output will be system average frequency. The input-output relationship could be formulated as follows,

$$H(z^{-1}) = \frac{\Delta f}{\Delta P_e} = \frac{b_0 + b_1 z^{-1} + \dots + b_m z^{-m}}{1 + a_1 z^{-1} + \dots + a_n z^{-n}}$$

Where  $n, m$  represents the order of the denominator and the numerator.

After estimating the linear model between the power imbalances and the frequency and converting into continuous time model, a step response is simulated. Based on the swing equation, inertia is estimated by calculating the RoCoF of the step response. A low-pass filter is applied to the step response to filter out high-frequency oscillations. RoCoF is estimated by the slope of the linear regression within each sliding window. The length of the sliding window should be selected considering the dynamic characteristics of the study system. The highest RoCoF will be used to estimate the inertia using the swing equation.

## III. IMPACT FACTORS OF PROBING-BASED METHOD

This section will discuss some of the impact factors that may affect the performance of the proposed probing-based inertia estimation in field applications. A summary of the considered factors is shown in Figure 2.

### 1) Load fluctuations

In normal operations, power system loads are constantly fluctuating, which cause system frequency constantly changing around nominal frequency. This ambient frequency noise could affect the accuracy of the inertia estimation using probing-based method. If the frequency deviation caused by the probing signal is too small, it may be masked by the ambient frequency

This work is under the DOE SETO's SAPPHIRE project led by NREL and CURENT at University of Tennessee.

variations, which makes it difficult for the system identification procedure. Therefore, it is important to investigate the impacts

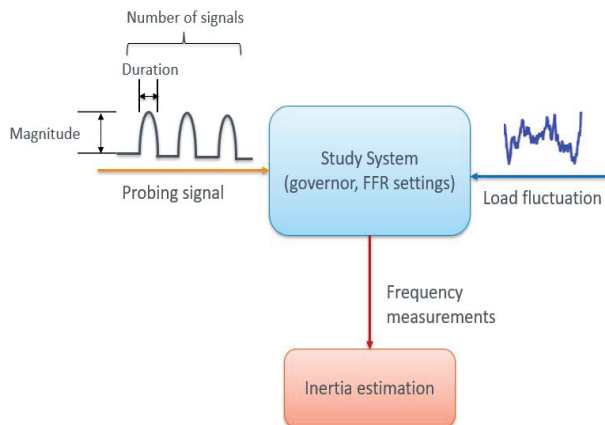


Figure 2 Impact factors of the probing-based method

of system ambient noise on the performance of the proposed probing-based method.

### 2) Shape of probing signal

Different types of probing signal with different magnitude and duration could excite system dynamics within different frequency range, which could affect the identified model and the simulated step response. The frequency spectrum of a suitable probing signal should be concentrated within the frequency range of interest.

### 3) Number of injected probing signals

In a probing test period, a series of identical probing signals could be injected consecutively. Instead of estimating the inertia based on a single probing injection, it may be helpful to average over a number of estimates within a short period of time because some of the uncertainties caused by the random load fluctuations could be canceled out. This could compensate for ignoring the load fluctuations when using the swing equation to estimate system inertia.

### 4) Settings of frequency response control

Apart from inertial response, there are other types of frequency response provided by the resource in the system following the power imbalances. Primary frequency responses provided by the synchronous generation through the droop control in the turbine governors are the main contributor of arresting system frequency at the nadir point. This type of responses acts slower than the inertial response, usually in several seconds. It is important to study the impacts of the governor control on the inertia estimation results. In addition, there is a growing number of IBRs that can provide FFR in the form of synthetic inertia and P-f droop with a response time less than 50ms. FFR control could influence the inertia estimation result, making it an equivalent inertia that includes the contribution from both synchronous resources and IBRs.

## IV. CASE STUDY

This section will present case study results of validating the proposed probing-based inertia estimation method using the 50-bus simulation model of Kauai island. Table I shows the inertia and governor settings of the synchronous plants.

Table I Synchronous plant settings

Plant Name	MBase (MVA)	Inertia Constant (s)	Governor deadband (mHz)	Governor Droop(%)
1	11.7	2.0	0	20
2	48	1.2	100	5
3	2.22	1.0	/	/
4	1.25	1.0	/	/
5	7.47	1.5	/	/
6	4.5	1.0	/	/

The theoretical inertia of the system could be calculated by summing up the kinetic energy in all the synchronous generation.

### A. Validation in ideal scenario without noise

To validate the effectiveness of the proposed method, a Hann signal with a peak magnitude of 0.75 MW and a duration of 2s is injected at the active power reference of the on Kauai island. The definition of the Hann signal is as follows,

$$Hann(t) = \begin{cases} \frac{1}{2} \left[ 1 - \cos\left(\frac{2\pi t}{T}\right) \right], & t \leq T \\ 0, & t > T \end{cases}$$

### 1) Governor control enabled, FFR control disabled

In this scenario, governor control of the synchronous plants is enabled and FFR from BESSs are disabled. The step response of the identified model is shown in Figure 3. A low-pass filter is applied to filter out the high-frequency components. A sliding window of 0.2s is applied to calculate the initial RoCoF. The theoretical inertia calculated from Table I is 102.1 MVA\*s, while the inertia estimated from the step response is 100.2 MVA\*s, which is very close to the ground

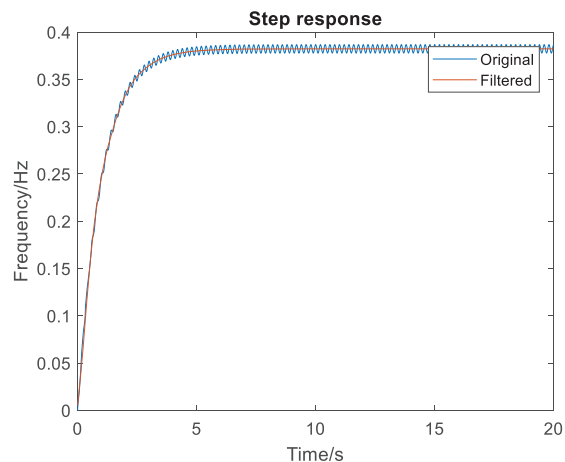


Figure 3 Step response of the identified model

truth. It shows that governor control does not have much impact on the performance of the method because inertia is estimated using the responses within a very short time period, when the effects from the governor control is limited.

2) Both governor control and FFR control enabled  
 In this scenario, the FFR control from two IBRs in the system are enabled. A P-f droop control strategy with 100mHz deadband is implemented to provide FFR. Figure 4 shows a comparison of system frequency response between the cases of disabling and enabling FFR control when using a Hann signal of 0.75 MW as the probing signal. It shows that system frequency disturbances are lower due to the additional support from FFR control. The inertia estimated with enabled FFR control is 148 MVA\*s, which is higher than the theoretical value. The difference could be considered as the contribution of FFR control to the equivalent inertia in this specific condition.

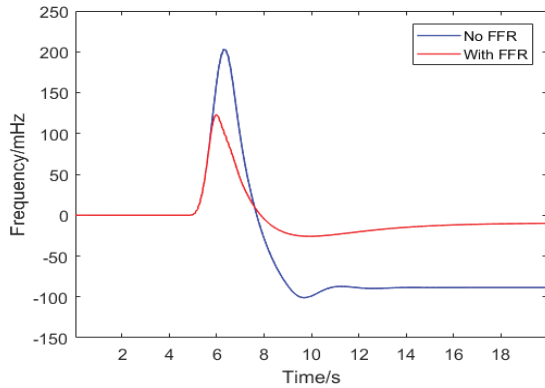


Figure 4 Comparison of frequency with and without FFR

### B. Validation in noisy scenarios

To mimic the ambient frequency noise in the Kauai island system, load fluctuations modeled by Gaussian noise are injected at the load buses in the simulation model. This study collected frequency measurements of the Kauai island captured by Universal Grid Analyzer (UGA) devices developed by FNET GridEye and calculated the ambient noise level. Then, to match the real measurements in field applications, the magnitude of the injected Gaussian noise is adjusted

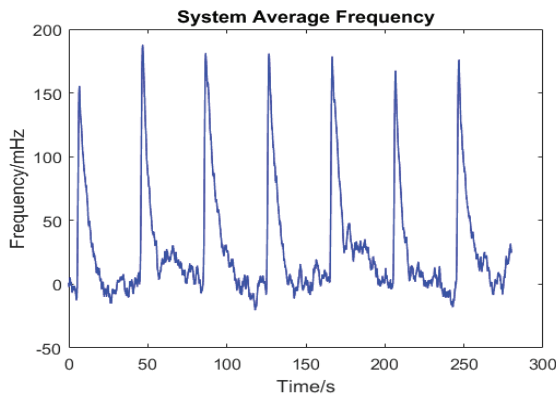


Figure 5 System average frequency during probing

simultaneously at all the load buses until the simulated ambient frequency noise level is close to the noise level calculated from the UGA data.

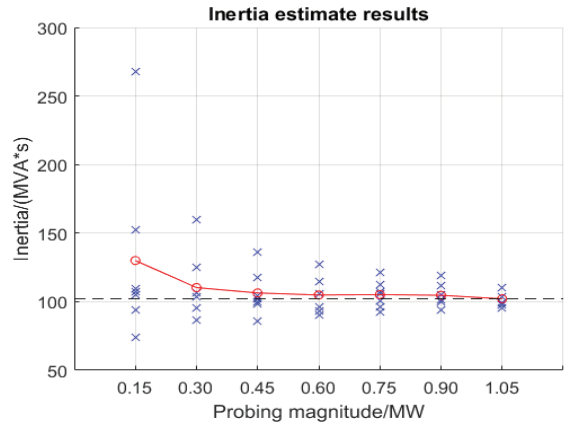


Figure 6 Comparison of different probing magnitude

To improve the accuracy of the inertia estimation in presence of load fluctuations, this study injects a series of probing signal at an interval of 40s over a time range of 300s. An example of the system average frequency deviation during the probing test is shown in Figure 5. The frequency spikes correspond to the frequency transients caused by the probing injection.

To study the impacts of different magnitude of probing signal on the performance of the inertia estimation under noisy conditions, a series of experiments are implemented by using the Hann signal with a duration of 2s as the probing signal. Governor control are enabled and FFR control from IBRs are disabled. The inertia estimates with different probing magnitude are compared in Figure 6. For each probing magnitude, the blue cross mark represents the single estimate from each probing signal injected during the probing test period. The red dot represents the average of all the single estimates from the series of probing signals injected. The dashed lines represent the theoretical system inertia. Several key findings could be summarized from this comparison,

1) It can be observed that with a higher probing magnitude, the average estimated inertia is more accurate. Also, the spread of all the estimates become more concentrated around the mean value as the probing magnitude increases. This is because a higher magnitude of MW injection could cause a larger frequency deviation in the system and weaken the impacts of load fluctuation on the estimation results.

2) It is helpful to average over a series of probing signals instead of estimating from a single probing injection. The average over multiple signals injected within a short period of time could cancel out some of the uncertainties caused by the load fluctuations.

3) The improvement of increasing probing magnitude become limited when the magnitude is large enough. However, higher probing magnitude also have the disadvantage of causing larger frequency disturbance in the system. The selection of a suitable probing signal for field applications

should consider the balance between the estimation accuracy and the impacts on system normal operation.

Table II shows a comparison of the estimation accuracy and the maximum frequency deviation caused by the probing between different types of probing signal. It can be observed that different types of probing signal also affect the accuracy of the inertia estimation, which could be caused by the difference in the frequency range of the system response excited by the probing signal. Generally, pulse signal with the same magnitude results in larger frequency disturbances in the system than Hann signal.

Table II Comparison of probing signals

Probing signal	Error (%)	Max freq deviation (mHz)
Hann, duration 2s, peak mag 0.75 MW	3.01	142
Pulse, duration 2s, 1s ramp-up, peak mag 0.75 MW	3.02	192
Pulse, duration 4s, 1s ramp-up, peak mag 0.75 MW	0.42	197

## V. CONCLUSION AND FUTURE WORK

This paper proposes a probing-based inertia estimation through PV-BESS plants in the Kauai island system. The proposed method is validated via simulation under different system conditions, considering the practical concerns in field applications, including ambient noise level, selection of probing signals and frequency response control settings. It is observed that a well-chosen probing magnitude and multiple probing injections during a short period of time could improve the accuracy of the inertia estimation accuracy. These key findings could help with the design of a suitable probing implementation plan in field applications.

For future work, the performance of the method will be tested under noisy conditions with different types of FFR strategies enabled. The team will also investigate the impact of the location of the probing injection on the inertia estimation results. In addition, hardware-in-loop tests and field demonstration of the proposed inertia estimation method will be implemented in the Kauai island grid in the future.

## REFERENCES

- [1] T. Inoue, H. Taniguchi, Y. Ikeguchi and K. Yoshida, "Estimation of power system inertia constant and capacity of spinning-reserve support generators using measured frequency transients," *IEEE Trans. Power Syst.*, vol. 12, no. 1, pp. 136-143, 1997.
- [2] D. Chassin, Z. Huang, M. Donnelly, C. Hassler, E. Ramirez and C. Ray, "Estimation of WECC system inertia using observed frequency transients," *IEEE Trans. Power Syst.*, vol. 20, no. 2, pp. 1190-1192, 2005.
- [3] S. Sharma, S. Huang and N. Sarma, "System inertia frequency response estimation and impact of renewable resources in ERCOT interconnection," in *IEEE Power Energy Soc. Gen. Meeting*, 2011.
- [4] P. Ashton, G. Taylor, A. Carter, M. Bradley and W. Hung, "Application of phasor measurement units to estimate power system inertia frequency response," in *IEEE Power Energy Soc. Gen. Meeting*, 2013.
- [5] P. Wall and V. Terzija, "Simultaneous estimation of the time of disturbance and inertia in power systems," *IEEE Trans. Power Del.*, vol. 29, no. 4, pp. 2018-2031, 2014.
- [6] M. Shamirzaee, H. Ayoubzadeh, D. Farokhzad, F. Aminifar and H. Haeri, "An improved method for estimation of inertia constant of power system based on polynomial approximation," in *Smart Grid Conf.*, 2014.
- [7] P. Ashton, C. Saunders, G. Taylor, A. Carter and M. Bradley, "Inertia estimation of the GB power system using synchrophasor measurements," *IEEE Trans. Power Syst.*, vol. 30, no. 2, pp. 701-709, 2015.
- [8] R. Panda, A. Mohapatra and S. Srivastava, "Online estimation of system inertia in a power network utilizing synchrophasor measurements," *IEEE Trans. Power Syst.*, vol. 35, no. 4, pp. 3122-3132, 2020.
- [9] D. Yang, B. Wang, G. Cai, Z. Chen, J. Ma, Z. Sun and L. Wang, "Data-driven estimation of inertia for multi-area interconnected power systems using dynamic mode decomposition," *IEEE Trans. Ind. Informat.*, 2020.
- [10] J. Pierre, D. Trudnowski and M. Donnelly, "Initial results in electromechanical mode identification from ambient data," *IEEE Trans. Power Syst.*, vol. 12, no. 3, pp. 1245-1251, 1997.
- [11] N. Zhou, J. Pierre, D. Trudnowski and R. Guttromson, "Robust RLS methods for online estimation of power system electromechanical modes," *IEEE Trans. Power Syst.*, vol. 22, no. 3, pp. 1240-1249, 2007.
- [12] J. Zhang and H. Xu, "Online identification of power system equivalent inertia constant," *IEEE Trans. Ind. Electron.*, vol. 64, no. 10, pp. 8098-8107, 2017.
- [13] K. Tuttleberg, J. Kilter, D. Wilson and K. Uhlen, "Estimation of power system inertia from ambient wide area measurements," *IEEE Trans. Power Syst.*, vol. 33, no. 6, pp. 7249-7257, 2018.
- [14] X. Cao, B. Stephen, I. Abdulhadi, C. Booth and G. Burt, "Switching Markov Gaussian models for dynamic power system inertia estimation," *IEEE Trans. Power Syst.*, vol. 31, no. 5, pp. 3394-3403, 2016.
- [15] J. Schiffer, P. Aristidou and R. Ortega, "Online estimation of power system inertia using dynamic regressor extension and mixing," *IEEE Trans. Power Syst.*, vol. 34, no. 6, pp. 4993-5001, 2019.
- [16] F. Allella, E. Chiodo, G. Giannuzzi, D. Lauria and F. Mottola, "Online estimation assessment of power systems inertia with high penetration of renewable generation," *IEEE Access*, vol. 8, pp. 62689-62697, 2020.
- [17] Y. Bian, H. Wyman-Pain, F. Li, R. Bhakar, S. Mishra and N. Padhy, "Demand side contribution for system inertia in the GB power system," *IEEE Trans. Power Syst.*, vol. 33, no. 4, pp. 3521-3530, 2018.
- [18] J. Mauricio, A. Marano, A. Gomez-Exposito and J. Martine Ramos, "Frequency regulation contribution through variable-speed wind energy conversion systems," *IEEE Trans. Power Syst.*, vol. 24, no. 1, pp. 173-180, 2009.
- [19] "Sonar of the power grid: new inertia measurement tools planned for Great Britain's electricity system," National Grid ESO, 11th December 2020. [Online]. Available: <https://www.nationalgrideso.com/news/sonar-power-grid-new-inertia-measurement-tools-planned-great-britains-electricity-system>.